The International Journal of Advanced Manufacturing Technology (2020) 106:877–890
https://doi.org/10.1007/s00170-019-04639-5

ORIGINAL ARTICLE

Chatter detection in milling processes using frequency-domain Rényi entropy

ZaoZao Chen[1] · ZhouLong Li[1] · JinBo Niu[1,2] · LiMin Zhu[1]

Received: 27 June 2019 / Accepted: 4 November 2019 / Published online: 30 November 2019

Abstract
Chatter is a kind of self-excited vibration and causes negative effects in machining processes. This paper presents a practical method to identify the chatter with cutting force signals in milling processes. Since the spectrum of the chatter signal exhibits discrete spectral lines around the chatter frequencies and the Rényi entropy is an effective index to characterize the randomness of data series, the frequency-domain Rényi entropy is proposed as a chatter indicator. As the chatter severity level grows, the signal components at the chatter frequencies become more and more significant, which means a reduction of the randomness of the spectral series. As a result, the value of the Rényi entropy-based indicator decreases rapidly at the onset of the chatter. In order to eliminate the interference of the normal signal components, i.e., the spindle speed-related frequency components, the spectrum is preprocessed to filter out those components first. Various milling experiments are conducted. The results show that the value of the proposed indicator changes sharply at the onset of chatter in various milling conditions with different spindle speeds and cutting depths. Also, the proposed indicator is compared with the commonly used Shannon entropy-based indicator and verified to have a larger difference between the stable and chatter statuses and is higher sensitivity to the chatter.

Keywords Chatter detection · Frequency analysis · Rényi entropy · Cutting force signal

1 Introduction

Various vibrations exist in milling processes, generating from the interactions between the cutting tool and the workpiece. Regenerative chatter is a kind of self-excited vibration, leading to many machining problems, such as poor surface quality, dimensional errors, severe noise, and shorter tool life. In order to prevent the occurrence of the chatter, operators have to select conservative cutting parameters by trial and error, including the feed rate, spindle speed, and cutting depth, which limit machining productivity inevitably. Then, researchers utilize analytical methods to model the machining process and search for the optimal chatter-free parameters with high machining efficiency. Some profound theories have been proposed by Budak and Altintas [1], Quintana and Ciurana [2], etc. So far, the stability lobe diagram based on these theories has been widely used to obtain the proper cutting parameters. However, owing to the environmental interference, complex cutting conditions and model simplification errors [3], chatter prediction may be inaccurate and unable to be accepted in industry. Therefore, the strategy of online cutting state monitoring is proposed to avoid the chatter while maintaining high machining efficiency. Since the transition process from the stable state to the chatter state has a short duration, detecting chatter at an early stage is a challenging task for researchers.

Recent years, some methods for online chatter identification have been proposed. Nearly all of these methods involve three steps, including signal acquisition, signal processing, and status recognition. As for signal acquisition, various sensors are utilized in milling processes, such as acceleration sensors [4], force sensors [5], displacement sensors [6], current sensors [7], and audio sensors [8]. In addition, multiple sensors are employed simultaneously to obtain more accurate

Electronic supplementary material The online version of this article (https://doi.org/10.1007/s00170-019-04639-5) contains supplementary material, which is available to authorized users.

✉ LiMin Zhu
zhulm@sjtu.edu.cn

[1] State Key Laboratory of Mechanical System and Vibration, School of Mechanical Engineering, Shanghai Jiao Tong University, Shanghai 200240, China

[2] Key Laboratory for Precision and Non-traditional Machining Technology of Ministry of Education, Dalian University of Technology, Dalian 116024, China

results [9]. As for signal processing, the time domain analysis, frequency domain analysis, and time-frequency analysis are applied to extract the chatter features from the monitored signals and construct the indices for machining status classification. Methods based on the time domain analysis usually have the advantages of lower computation complexity and less data required. Ye et al. [10] proposed the coefficient of variation (i.e., the ratio of the standard deviation to the mean) of the root mean square sequence for chatter identification. Lajmert et al. [11] employed the recurrence plot technique to find the initial point of chatter vibrations. Jia et al. [12] adopted a synthetic criterion integrating the time-domain standard deviation and one-step autocorrelation function for early chatter recognition. Although these methods show strengths in processing time, more researchers prefer detection techniques depending on the frequency and time-frequency analysis, since chatter is characterized by the changes of frequency and energy distribution [13]. When the machining state transfers from a steady one to the chatter state, the local peaks in the frequency domain become more significant at the chatter frequencies than those at the cutting tool's rotation frequency and its harmonics. Zhang et al. [14] introduced an approach using the Fast Fourier transform (FFT) to preprocess signals monitored and extract the feature vectors for cutting chatter monitoring. Shao et al. [15] established a chatter recognition technology based on machine learning, and the features applied in the learning model were extracted from vibration signals with the FFT. To utilize the information of both time and frequency domain simultaneously, time-frequency analysis techniques, mainly including the wavelet analysis and Hilbert-Huang transform (HHT), are exploited in chatter monitoring. Zhang et al. [13] decomposed the force signal into two groups of sub-signals using the variational mode decomposition and wavelet packet decomposition, respectively; then, the energy entropies were calculated with these sub-signals to identify the milling chatter. Cao et al. [16] presented a method for chatter identification of the end milling process based on the wavelet package transform (WPT) and Hilbert–Huang transform (HHT). Cabrera et al. [17] proposed an approach relying on the wavelet analysis of cutting force signals to identify chatter vibrations of milling processes. Although the wavelet analysis technology is useful, it is inconvenient to choose the optimal wavelet basis and decomposition levels. Also, these parameters need to be adjusted when processing signals from different cutting conditions. To overcome this difficulty, the empirical mode decomposition (EMD) is exploited for signal processing. It is a self-adaptive analysis method without specifications. The nonlinear and nonstationary signal can be decomposed into a set of complete and almost orthogonal components named intrinsic mode functions (IMF) directly [18]. Considering the mode mixing problem existing in the EMD, an improved method called ensemble empirical mode decomposition (EEMD) was proposed and has been widely used in chatter recognition accompanied with the wavelet analysis, the Hilbert transform (HT), and other signal processing techniques. Liu et al. [7] decomposed the measured signals into IMFs with the EMD first, and then the IMFs related to chatter were selected to calculate the energy index and kurtosis index for chatter identification. Fu et al. [19] proposed an energy aggregation characteristic-based method for online chatter detection with a series of IMFs decomposed by the EEMD. Wan et al. [20] defined the variance ratio of the filtered signal series to the original signal series as a chatter indicator, and the dominant chatter frequency was estimated using the EEMD and HT. Liu et al. [21] selected the IMFs changing consistently with the power spectrum for signal reconstruction, and then the mean value and standard deviation of the reconstructed signal's HHT spectrum were extracted as the feature vectors. Wei et al. [22] applied the EEMD to decompose the measured cutting force into multiple IMFs first, and then the energy ratio of the dominant frequencies was calculated to identify the chatter. It is worth mentioning that the spectrum of vibrations when chatter occurs will show multiple frequencies spread on the right and left sides of the chatter frequency [9]. Hence, the sub-signals obtained using the EEMD or WPD are unable to contain all the chatter-related components.

At last, the milling status needs to be determined with the processed signals. Various indicators have been proposed and verified to be useful in chatter detection. Ji et al. [4] took the multi-indicators, including the standard deviation, power spectral entropy, and fractal dimension, as the input characteristic vectors to obtain a chatter identification model. Cao et al. [23] constructed two nonlinear dimensionless indices, i.e., C_0 complexity and power spectral entropy, from the sensitive IMFs as the chatter indicators. Chen et al. [24] selected the one-step autocorrelation function and impulse factor from ten time-domain and four frequency-domain features to identify the transition from the stable to the unstable milling state. In recent years, several intelligent approaches are applied in machining status classification, such as the logistic regression [5], support vector machine (SVM) [25], hidden Markov model (HMM) [26], and neural networks (NN) [27].

In this work, the problem of chatter feature extraction is revisited from the perspective of frequency-domain information entropy. It is known that the spectrum of the chatter signal exhibits spectral lines around the chatter frequencies. As the chatter progresses, these spectral lines become significant, which means a reduction of the randomness of the spectral series from the point of view of statistics. Since the Rényi entropy is an effective index to characterize the randomness of data series, the frequency-domain Rényi entropy is proposed as a chatter indicator. It only relies on the FFT. Compared with those based on the WPT and HHT, the proposed indicator needs not to specify any additional parameters and is computationally efficient. The rest of paper is organized as follows. The milling force model and generalized Rényi

entropy are introduced in Sect. 2. Section 3 presents the experimental setup and signal acquisition. The results and discussions are given in Sect. 4. Finally, the conclusion is summarized in Sect. 5.

2 Feature extraction

2.1 Milling force model

In this paper, the milling force signals are selected for chatter identification. With the milling force model established by Altintas et al. [28], the changes of milling forces when the cutting status transfers from the stable one to the chatter one can be revealed. The schematic of the milling force model is shown in Fig. 1. As established in ref.[28], the resulting regenerative dynamic chip thickness caused by vibrations is

$$\mathrm{h}_i(t) = (\Delta x(t)\sin(\phi_i(t)) + \Delta y(t)\cos(\phi_i(t)))m(\phi_i(t)) \quad (1)$$

where $\Delta x(t)$ and $\Delta y(t)$ are the differenced vibrations in the x and y directions respectively, and $\phi_i(t)$ is the instantaneous angular position of the ith tooth. The function $m(\phi_i(t))$ indicates whether the ith tooth is in or out of the cut. If the tooth is in the cut, $m(\phi_i(t))$ is set as 1. Otherwise, $m(\phi_i(t))$ is 0. Considering the static chip thickness, the whole chip thickness becomes

$$H_{\mathrm{i}}(t) = \Big(c\sin(\phi_i(t)) + \Delta x(t)\sin(\phi_i(t)) + \Delta y(t)\cos(\phi_i(t))\Big)m(\phi_i(t)) \quad (2)$$

where c is the feed per tooth. The tangential force $f_i^t(t)$ and the radial force $f_i^{\mathrm{r}}(t)$ acting on the ith tooth can be expressed as

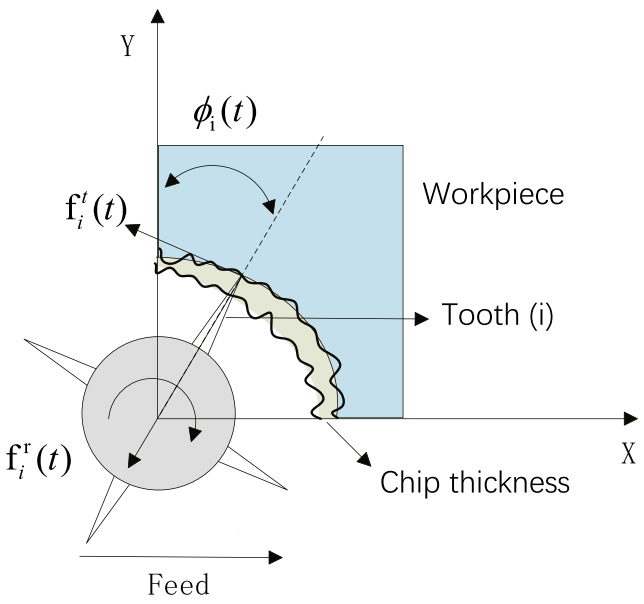

Fig. 1 The schematic of the milling force model

$$f_i^t(t) = K_t a H_i(t),\ f_i^r(t) = K_r f_i^t(t) \quad (3)$$

where K_{t} and K_{r} are constant cutting force coefficients, and a is the axial depth. Then, the cutting forces in the x and y directions can be obtained as

$$F_{\mathrm{i}}^x(t) = -f_i^t(t)\cos(\phi_i(t)) - f_i^r(t)\sin(\phi_i(t)) \quad (4)$$

$$F_{\mathrm{i}}^{\mathrm{y}}(t) = f_i^t(t)\sin(\phi_i(t)) - f_i^r(t)\cos(\phi_i(t)) \quad (5)$$

The total milling force is the summation of the cutting forces acting on all the teeth.

$$F_{\mathrm{x}}(t) = \sum_{i=1}^{N} F_i^x(t)\ ,\ \ F_y(t) = \sum_{i=1}^{N} F_i^y(t) \quad (6)$$

where N denotes the number of teeth. Now, $F_{\mathrm{x}}(t)$ is taken for example. As pointed out by Ma et al. [29], the Fourier series expansion of $F_{\mathrm{x}}(t)$ consists of the tooth passing frequency, the chatter frequency, and their harmonics.

$$F_{\mathrm{x}}(t) = \sum_{i=-\infty}^{\infty} F_i e^{ji\omega_T t} + \sum_{i=-\infty}^{\infty}\left(C_i^+ e^{j(\omega_c + i\omega_T)t} + C_i^- e^{j(-\omega_c - i\omega_T)t}\right) \quad (7)$$

where ω_T is the tooth passing frequency, ω_{c} is the chatter frequency, j denotes the imaginary unit, and F_i, C_i^+, C_i^- denote the amplitudes of the corresponding frequency components, respectively. The second part in Eq. (7) represents the chatter-related components significant in the proposed method. Considering the finite energy contained in the signal and environmental disturbance, the Fourier series expansion of $F_x(t)$ can be further expressed as [29]

$$F_x(t) \approx \sum_{i=-N_1}^{N_1} F_i e^{ji\omega_T t} + \sum_{k=-N_2}^{N_2} C_k^+ e^{j(\omega_c + k\omega_T)t} + \sum_{k=-N_2}^{N_2} C_k^- e^{j(-\omega_c - i\omega_T)t} + W(t) \quad (8)$$

where $W(t)$ denotes the additive Gaussian white noise, and N_1 and N_2 are the numbers of the significant harmonics. After filtering out the components corresponding to the tooth passing frequency and its harmonics, the Fourier series expansion of the residual cutting force signal $F_x(t)$ is given by

$$\widetilde{F_x(t)} \approx \sum_{k=-N_2}^{N_2} \left(C_k^+ e^{j(\omega_c + k\omega_T)t} + C_k^- e^{j(-\omega_c - k\omega_T)t} \right) + W(t) \quad (9)$$

When the cutting state is stable, C_j^+ and C_j^- are small and $\widetilde{F_x(t)}$ is dominated by $W(t)$. Therefore, the energy of $\widetilde{F_x(t)}$ are almost evenly distributed in the frequency domain. When the chatter occurs, the chatter-related components grow rapidly and begin to dominate $\widetilde{F_x(t)}$. As the chatter severity level increases, the frequency components of $\widetilde{F_x(t)}$ become significant at the chatter-related frequencies, i.e.,$\omega_c + k\omega_T$ and $-\omega_c - k\omega_T (k = -N_2, -N_2 + 1, \ldots, N_2)$. Although it is difficult to determine accurately the chatter frequency ω_c in the actual machining process, the characteristics of the frequency-domain energy distribution can be utilized in chatter detection.

2.2 The generalized Rényi entropy

According to the milling model in Sect. 2.1, it is known that the chatter force signals in milling processes contain mainly the frequency components at the chatter frequencies. Meanwhile, the entropy is an index to characterize the randomness of data. A larger entropy denotes that the distribution of data is comparatively even and uncertain, while a smaller value indicates that the distribution uncertainty is less. When the entropy is employed to characterize the frequency and energy distribution of cutting forces in the frequency domain, its value would exhibit much differences for the stable and chatter states. Therefore, the frequency-domain entropy is a potential index for chatter monitoring. In fact, the well-known Shannon entropy has been adopted to identify chatter in the previous works of Yang et al. [3], Ji et al. [4], Ding et al. [5], and Zhang et al. [13]. All of these studies show that the results are promising. In this paper, the Rényi entropy, the generalized form of the Shannon entropy, is applied and shows better performance in chatter detection.

2.2.1 Definition

Assume a complete probability set of a random event X is $p = \{p_1, p_2, ..., p_n\}$, the summation of whose probabilities is 1. Then, the generalized Rényi entropy, parameterized by order α, is defined as [30]:

$$H_\alpha(p) = \frac{1}{1-\alpha} \log_2 \frac{\sum_i p_i^\alpha}{\sum_i p_i} \quad \alpha > 0, \alpha \neq 1 \quad (10)$$

The Rényi entropy is a dimensionless indicator, and it yields a larger result when all values of the probability set are almost equal to each other, while it yields a smaller result if only a few values are large and others keep small. If we construct a non-negative data set $\zeta = \{\zeta_1, \zeta_2, ..., \zeta_N\}$ satisfying the conditions aforementioned using the spectrum of cutting force signals, then the Rényi entropy can be adopted to characterize the energy distribution of the signal in the frequency-domain and regarded as an indicator for chatter detection.

Different α in Eq. (10) can be selected, and it is worth mentioning that the well-known Shannon entropy could be recovered from $\lim_{\alpha \to 1} H_\alpha$. Since the total probabilities are equal to 1, it can be proved that the range of the Rényi entropy is always $[0, \log_2 n]$ for any α. However, the performance of the Rényi entropy changes with different α selected. As verified by Tao et al. [30], the Rényi entropy with a larger α is more sensitive to the energy concentration and thus is more favorable for condition monitoring. In other words, if we choose the α larger than 1, the indicator would be more sensitive than the commonly used Shannon entropy indicator. However, the Rényi entropy with a larger α is easier to be disturbed by spurious vibration signals. In order to satisfy the requirements of high sensitivity to the abnormal chatter and robustness against the environment disturbance, α is set as 3 in this research.

2.2.2 The indicator calculation

Firstly, the windowed FFT is applied to the sampled signal to obtain the amplitude spectrum. Secondly, to eliminate the interference of the spindle speed-related frequency components, the amplitudes of the spectral lines at these frequencies are imposed to be 0. Thirdly, the resulting sequence is normalized to satisfy the requirements of Eq. (10) and the Rényi entropy is calculated with the new data sequence finally. The detailed procedure is described as follows:

Step 1: Apply the windowed FFT to the sampled signal sequence $\{x(k), k = 1, 2, ..., N\}$ and get the amplitude spectrum sequence $\{X(k), k = 1, 2, ..., N\}$, where N is the length of the signal segment. The window function used here is the Hanning window. Since the amplitude spectrum is symmetrical, only half of the spectral lines are utilized in following steps.

Step 2: Set the amplitudes of the spectral lines corresponding to the spindle rotation frequency and its harmonics to be 0. In order to mitigate the influence of the power

leakage, for each frequency, totally three spectral lines, including the major spectral line with local maximum amplitude and its two neighbors, are processed.

Step 3: Normalize the modified amplitude spectrum sequence $\{Y(k), k = 1, 2, ..., \lceil N/2 \rceil\}$ obtained in step 2, resulting in the following data sequence

$$\beta_k = \frac{Y(k)}{\sum_k Y(k)}, k = 1, 2, \ldots \quad (11)$$

Apparently, β_k ranges between 0 and 1, and $\sum \beta_k = 1$.

Step 4: The frequency-domain Rényi entropy is calculated as

$$H_3 = \frac{1}{1-3} \log_2 \frac{\sum_{k=1}^{\lceil N/2 \rceil} (\beta_k)^3}{\sum_{k=1}^{\lceil N/2 \rceil} \beta_k} = -\frac{1}{2} \log_2 \sum_{k=1}^{\lceil N/2 \rceil} (\beta_k)^3 \quad (12)$$

Step 5: The result is normalized as follows to make the value of the indicator lie in the range [0,1] and independent of the length of the data sequence.

$$E = \frac{H_3}{\log_2 \lceil N/2 \rceil} \quad (13)$$

3 Experimental setup

Milling experiments were performed on a CNC milling machine for the validation of the proposed method as shown in Fig. 2. A two-fluted carbide flat end mill cutting tool with a diameter of 10 mm and overhang length of 80 mm was adopted in tests. The workpiece was a block of 6061 aluminum fixed on the platform dynamometer with bolts. The platform dynamometer was immobilized by pressure plates on the worktable and used for measuring cutting force signals. The signal was sampled with a data acquisition card and the sampling frequency was set as 20 kHz taking into account the spindle rotation frequency and its harmonic frequencies in the test. All the tests were conducted with coolant since the cutter was easily damaged when chatter occurred without coolant. Although additional environmental noise was added into the measured force signal with the coolant, the experimental data shows the influence can be ignored.

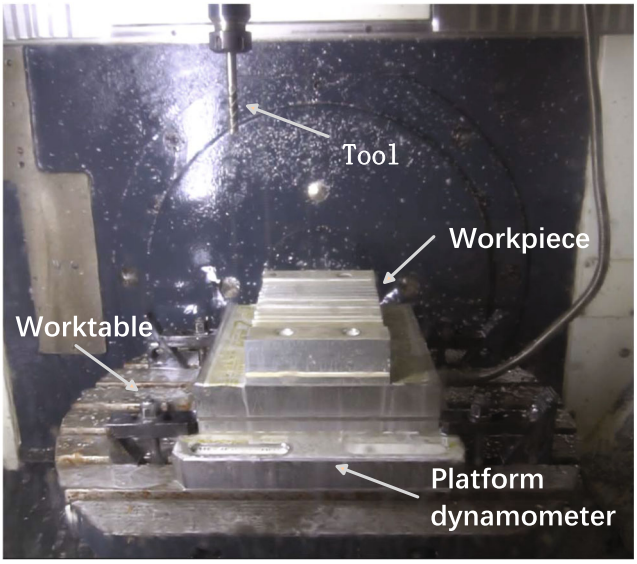

Fig. 2 The experimental setup

Since our aim is to detect the chatter at an early stage, data of the transition from the stable state to the chatter state should be captured in the tests to observe the variation of the indicator value at the onset of chatter. According to Ref. [1], the occurrence of chatter is directly associated with the cutting depth and spindle speed; thus, the axial cutting depth was decreased gradually when milling a slope in the tests as shown in Fig. 3. In this way, the cutting parameter changed continuously and the transition state was observed completely. It should be noted that since we decrease the cutting depth in the milling process, the collected data is inverted firstly in the data analysis process for the convenience of the explanation. The experimental parameters are summarized in Table 1. When choosing different spindle speeds, the ranges of cutting depth were also adjusted to ensure the occurrence of the transition status.

4 Results and discussions

In this section, the measured force signals are analyzed in both time and frequency domains to demonstrate the characteristics of different cutting states. Then, the effectiveness and robustness of the proposed indicator are validated. Finally, the proposed indicator is compared with the commonly used Shannon entropy-based indicator.

4.1 Data analysis

The useful periods of the measured signals in the experiments are extracted and presented in Fig. 4. It is clear that the amplitude of the cutting force in the time domain is relatively small in the stable status and grows up when chatter occurs. Since the variation trends of the force signals in different cases are

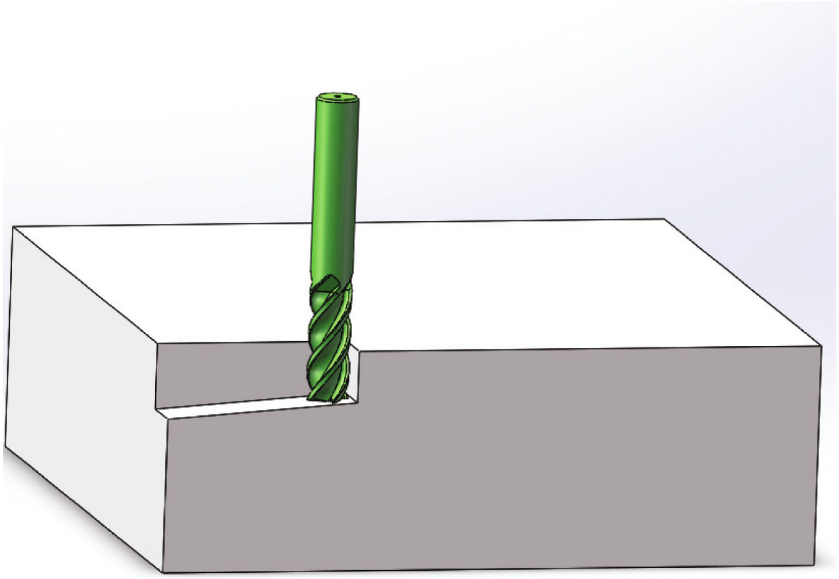

Fig. 3 The schematic of the cutting processes

similar, only the characteristics of the force signal in Case 1 are analyzed for concision.

Based on the force amplitude in the time domain, the whole milling process can be divided into three periods roughly, which are stable period, transition period, and chatter period. It is clear from Fig. 5 that the cutting force grows up with the development of chatter and the amplitude in the stable cutting condition is smaller than that in the chatter state obviously. Meanwhile, the duration of the transition state in Case 1 is short, just nearly 0.5 s.

When analyzing the characteristics of force signals in the frequency domain, a short segment of data is extracted from each period at first. The segments selected are indicated with red rectangles in Fig. 5. Then, the windowed FFT is utilized to convert the force signal from the time domain to the frequency domain. The spectrums of the three segments are shown in Figs. 6, 7, and 8. It can be seen that as the chatter develops, the amplitudes of spectral lines corresponding to the chatter components strengthen gradually, which shows the feasibility to detect the chatter in the frequency domain. It is worth mentioning that there is no obvious change of the force amplitude in segment 2 as compared with that in segment 1, while the spectral lines related to chatter components are evident in the frequency domain, which indicates the advantages of frequency domain analysis.

4.2 Chatter indicator

For the experimental data collected in Case 1, the Rényi entropy-based indicator calculated from the data segment in a moving window sliding along the time axis is shown in Fig. 9. The data length when calculating the indicator determines both the spectral resolution and computing time. Some significant spectral lines might be missed when the resolution is insufficient; thus, the length should not be too short. Meanwhile, the computing time will increase naturally with a longer length, which is harmful to monitor the chatter timely. Taking both factors into consideration, the segment length is set as 200 ms for index calculation in this research. It can be seen that the indicator value decreases sharply at the onset of chatter and there exists quite a big gap between the values corresponding to the stable and chatter states. As explained in Sect. 2, the entropy is an index to measure the randomness of data series. In the stable cutting condition, the signal energy is almost evenly distributed in the frequency domain, resulting in a bigger entropy at that stage. As the chatter begins to occur, the signal energy centralizes around the chatter frequencies gradually, which leads to the significant spectral lines and thus a decrease of the entropy. Figure 9 also shows that the indicator value changes earlier with a bigger changing rate than the force amplitude in the time domain, which indicates its higher sensitivity to the chatter.

Table 1 The cutting parameters for milling tests

No.	Spindle speed (rpm)	Radial depth (mm)	Feed rate (mm/min)	Cutting depth(mm)
1	5200	10	500	1.4–2.3
2	5600	10	500	1.4–2.3
3	6000	10	500	1.8–2.2
4	7400	10	500	1.2–1.8

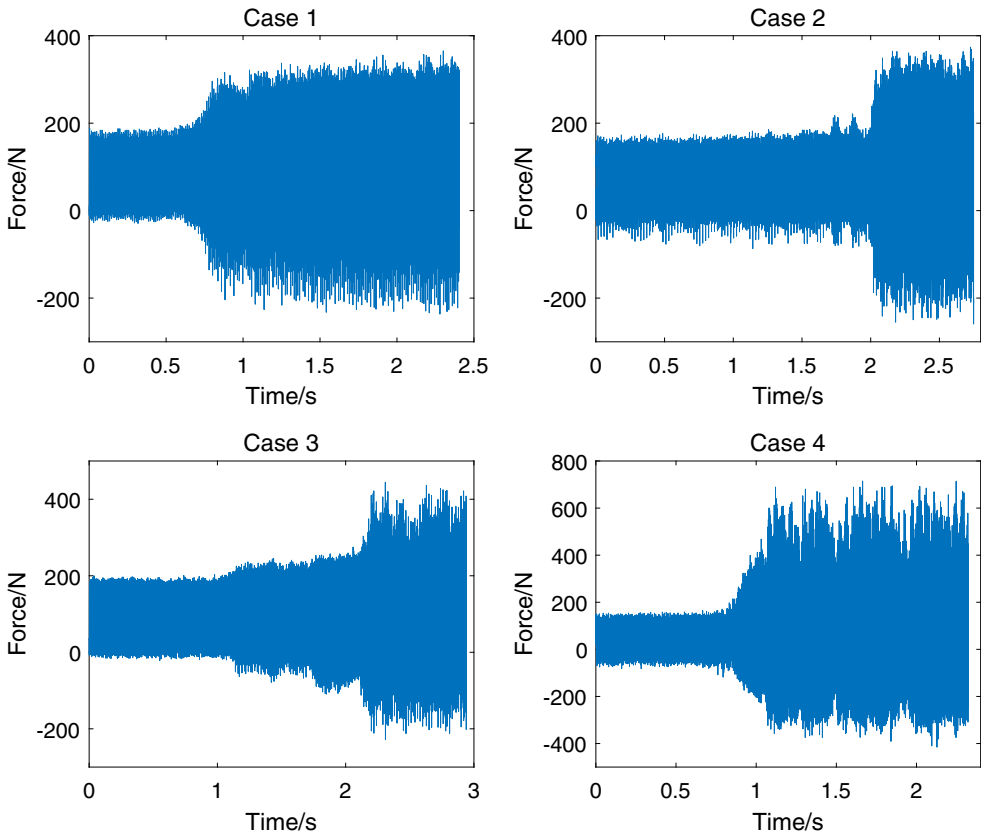

Fig. 4 The force signals of Cases 1–4 in the time domain

4.3 The robustness of the indicator

The experimental results of Case 1 have shown that the Rényi entropy-based indicator is capable of identifying the chatter at the early stage. In order to investigate its robustness, the experimental results of Cases 2–4 are presented. As displayed in Fig. 10, the indicator shows good performance in distinguishing milling states under all of these three different milling conditions and detects chatter at quite an early stage.

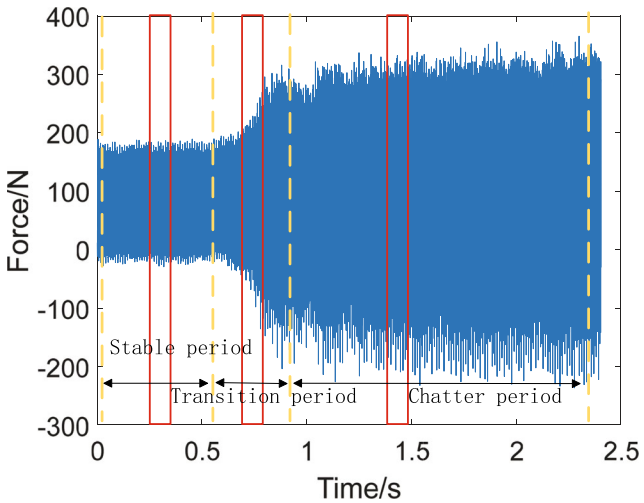

Fig. 5 The force signal of Case 1 in the time domain with a rough division of three periods.

In this sense, the Rényi entropy-based indicator possesses good robustness since it is effective in various milling conditions.

4.4 Comparison with the Shannon entropy

The Shannon entropy has been verified to be a good indicator for chatter identification by Ji et al. [4], Zhang et al. [13], Cao et al. [23], Liu et al. [31], Ji et al. [32], etc. In this subsection, the chatter detection performances of Shannon entropy and the proposed Rényi entropy are compared in detail. The four experimental cutting tests in Table 1 are used to evaluate these two indicators.

As shown in Fig. 11, the proposed Rényi entropy distinguishes different cutting statuses successfully for all cases, while the Shannon entropy fails for Case 4. The indicator values of Shannon entropy are too close to be distinguished for stable cutting and chatter periods in this cutting condition. In order to further compare the detection performance, these two indicators are evaluated in terms of variation range, sensitivity to chatter onset, and agility to detect chatter at the early stage.

Variation range According to Fig. 11, the Rényi entropy shows larger indicator value differences between the stable status and the chatter status than the Shannon entropy, which

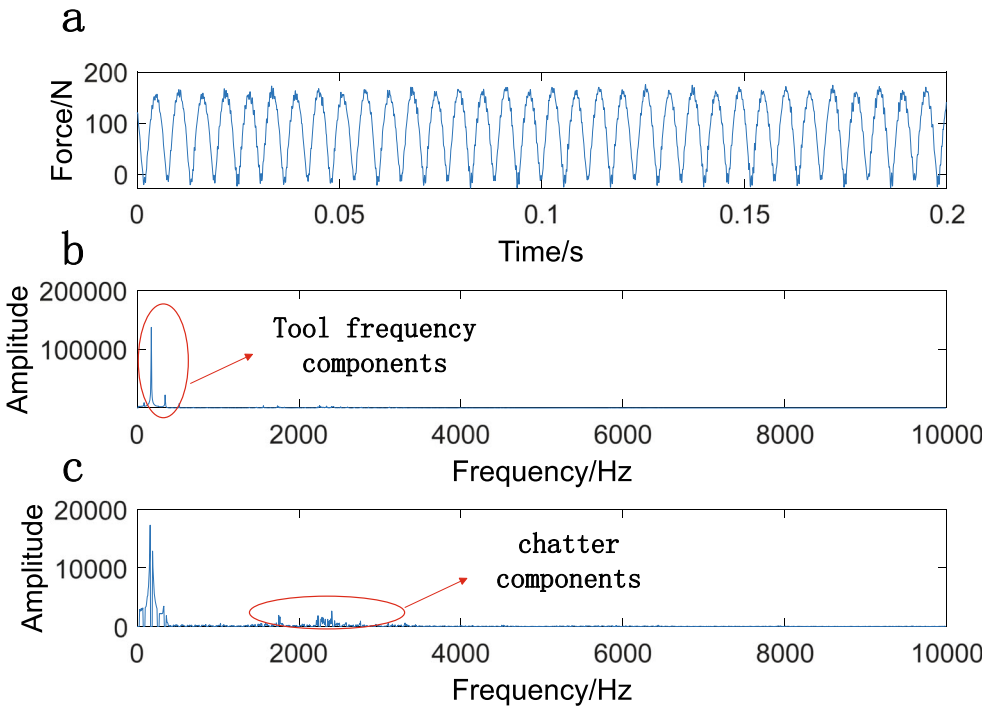

Fig. 6 The data of signal segment 1, corresponding to the stable state. **a** The force signal in the time domain. **b** The Fourier amplitude spectrum of the signal segment. **c** The amplitude spectrum after filtering the spindle speed-related frequency components in the frequency domain.

indicates that the Rényi entropy-based indicator may distinguish cutting statuses better with a lower probability of misjudging.

4.5 Sensitivity to the onset of chatter

As illustrated in Fig. 10, the indicator values will change at the onset of chatter; thus, the changing rate can be utilized to represent the indicator sensitivity. Assume an entropy sequence is $\{e(j), j = 1, 2, ...\}$, then the corresponding absolute changing rate can be defined as:

$$c(j) = \left|\frac{e(j+1) - e(j)}{e(j)}\right|, \quad j = 1, 2, \ldots \tag{14}$$

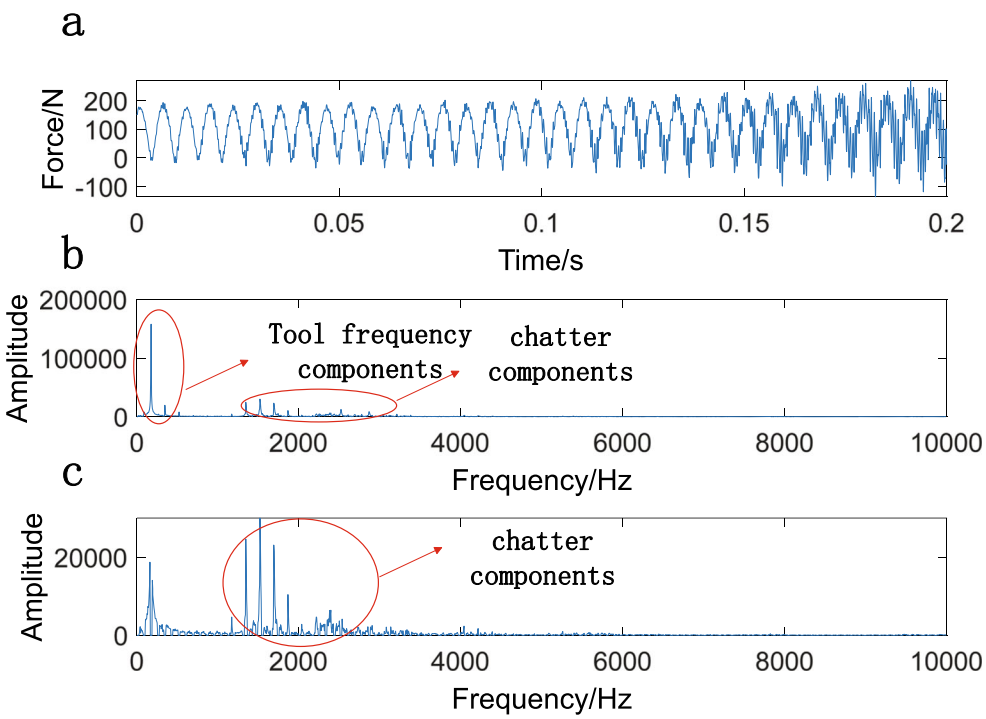

Fig. 7 The data of signal segment 2, corresponding to the transition state. **a** The force signal in the time domain. **b** The Fourier amplitude spectrum of the signal segment. **c** The amplitude spectrum after filtering the spindle speed-related frequency components in the frequency domain

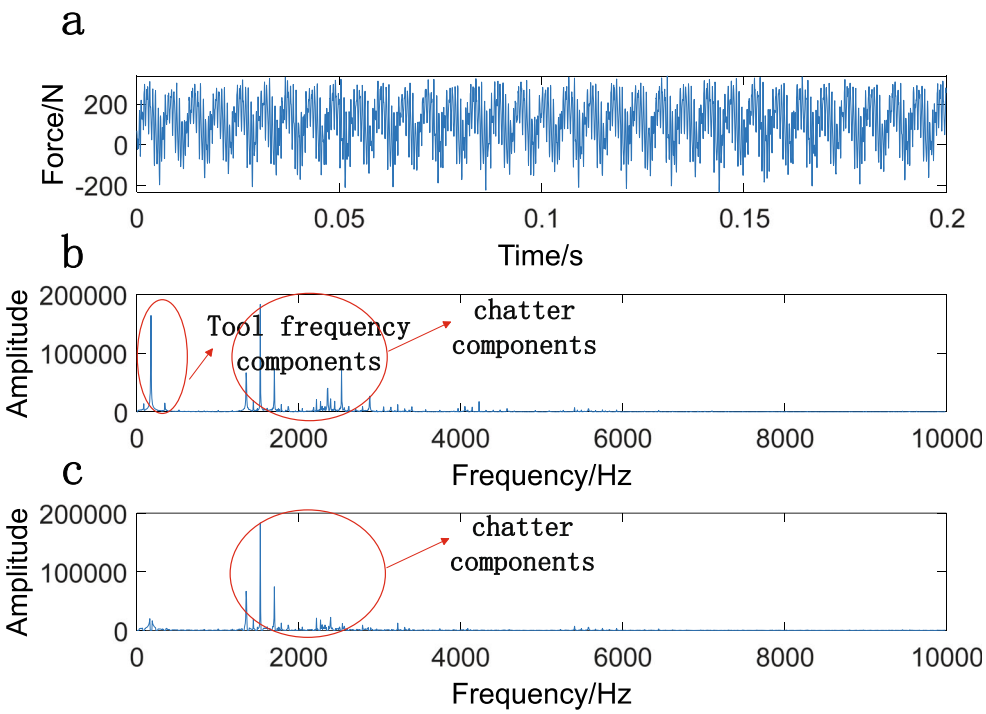

Fig. 8 The data of signal segment 3, corresponding to the chatter state. **a** The force signal in the time domain. **b** The Fourier amplitude spectrum of the signal segment. **c** The amplitude spectrum after filtering the spindle speed-related frequency components in the frequency domain

Since the onset of chatter occurs in the transition period, the changing rates in this period are calculated based on Eq. (14) for the Shannon entropy and the Rényi entropy-based indicators, respectively. As shown in Fig. 12, the absolute changing rate of the Rényi entropy is larger than that of the Shannon entropy at most time nodes, which indicates that it has higher sensitivity to the chatter.

Agility to detect chatter at the early stage It has been verified that the entropy-based indicator decreases when the chatter occurs. As presented in Fig. 13, the entropy value diminishes from the initial time and keeps constant after the final time. In practice, an alarm value can be preseted and once the indicator value is less than this one, the chatter is considered to occur and the

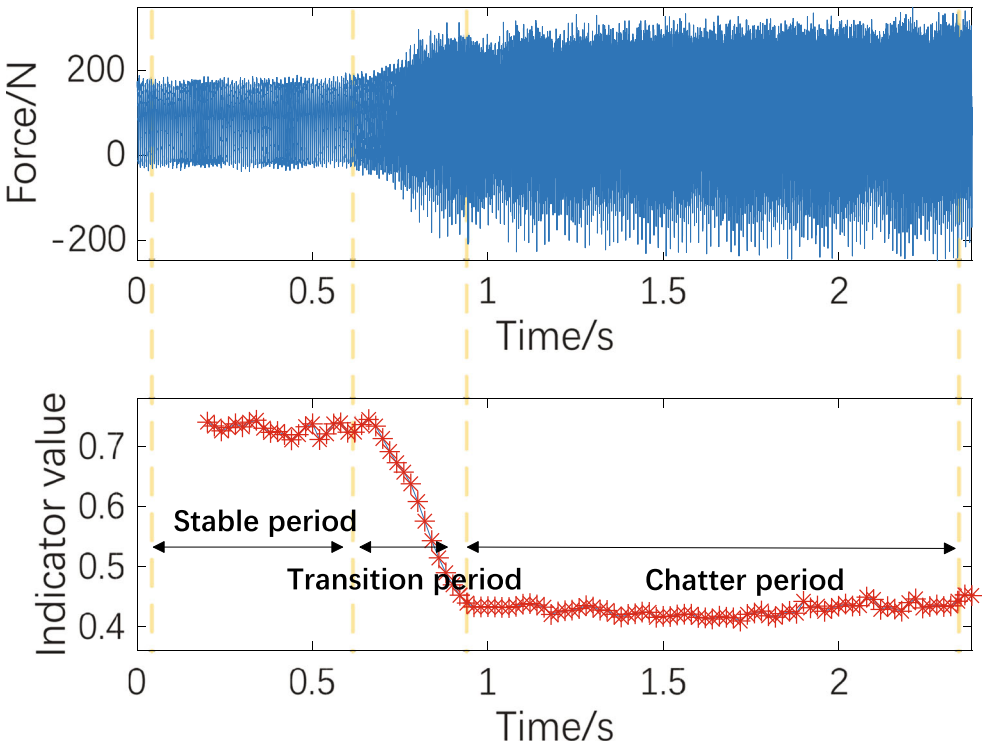

Fig. 9 The force signal in the time domain and the corresponding Rényi entropy indicator values of Case 1

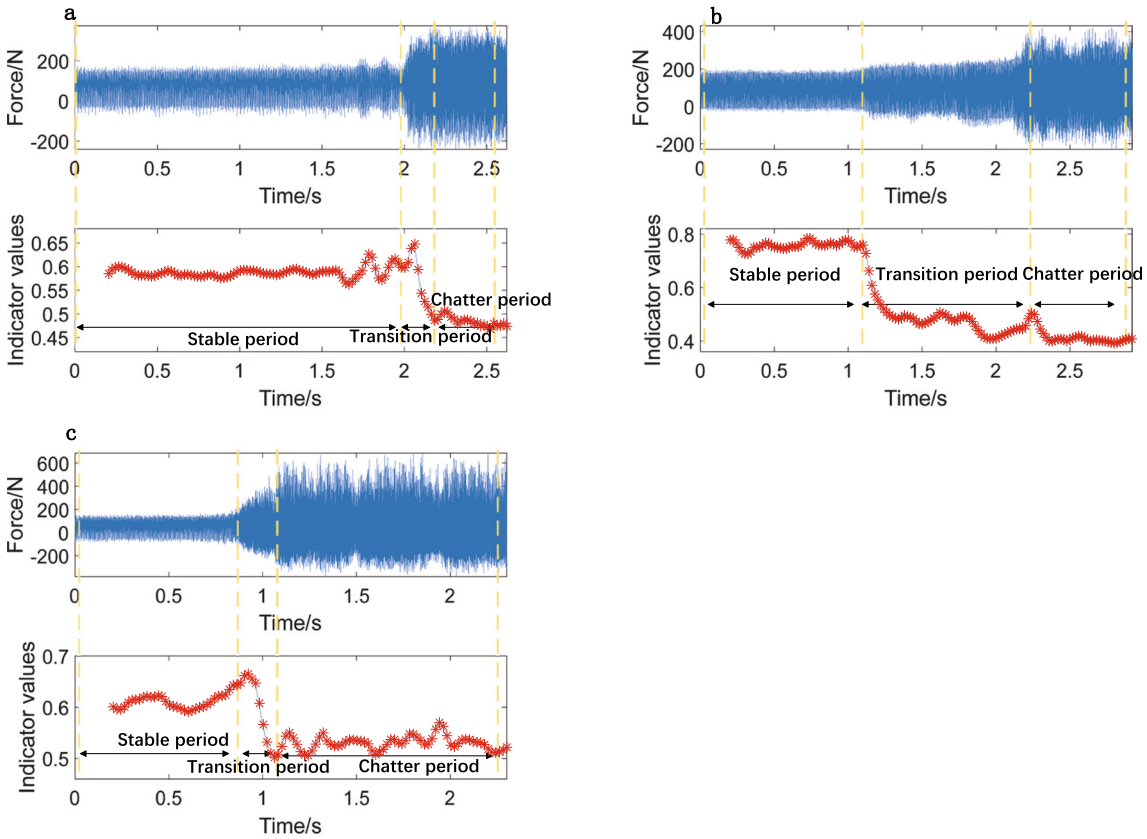

Fig. 10 The force signal in the time domain and the corresponding Rényi entropy indicator values of different cases. **a** Case 2. **b** Case 3. **c** Case 4

corresponding time can be defined as the trigger time. Obviously, the indicator possessing an earlier trigger time with the same alarm value shows better performance in chatter detection.

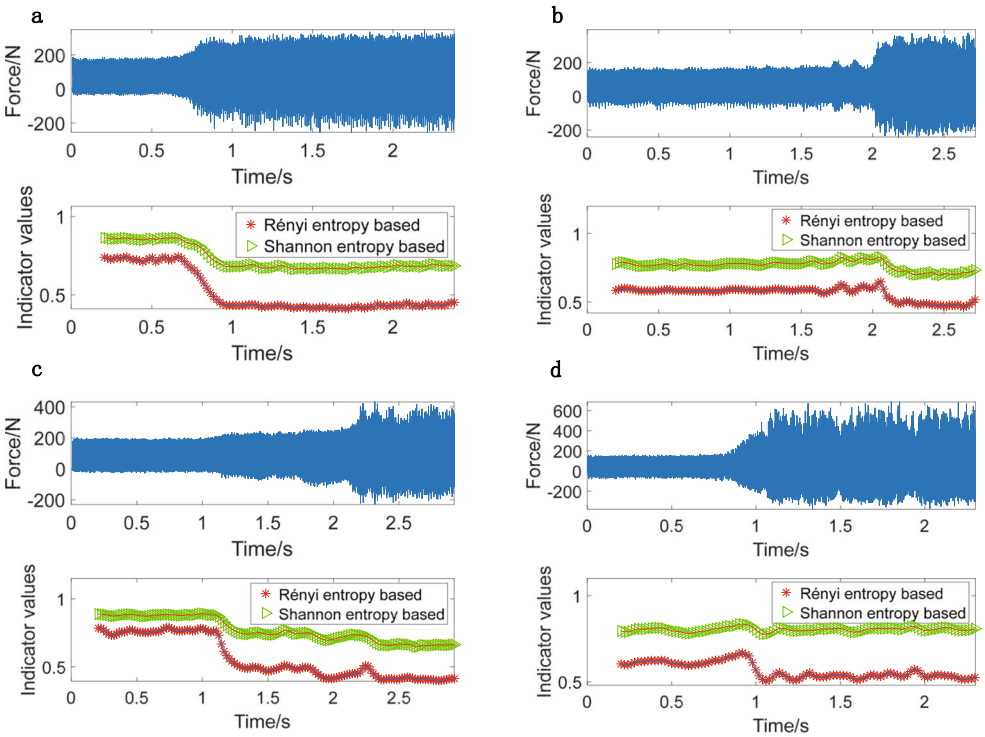

Fig. 11 The Rényi entropy and Shannon entropy indicators values of different cases. **a** Case 1. **b** Case 2. **c** Case 3. **d** Case 4

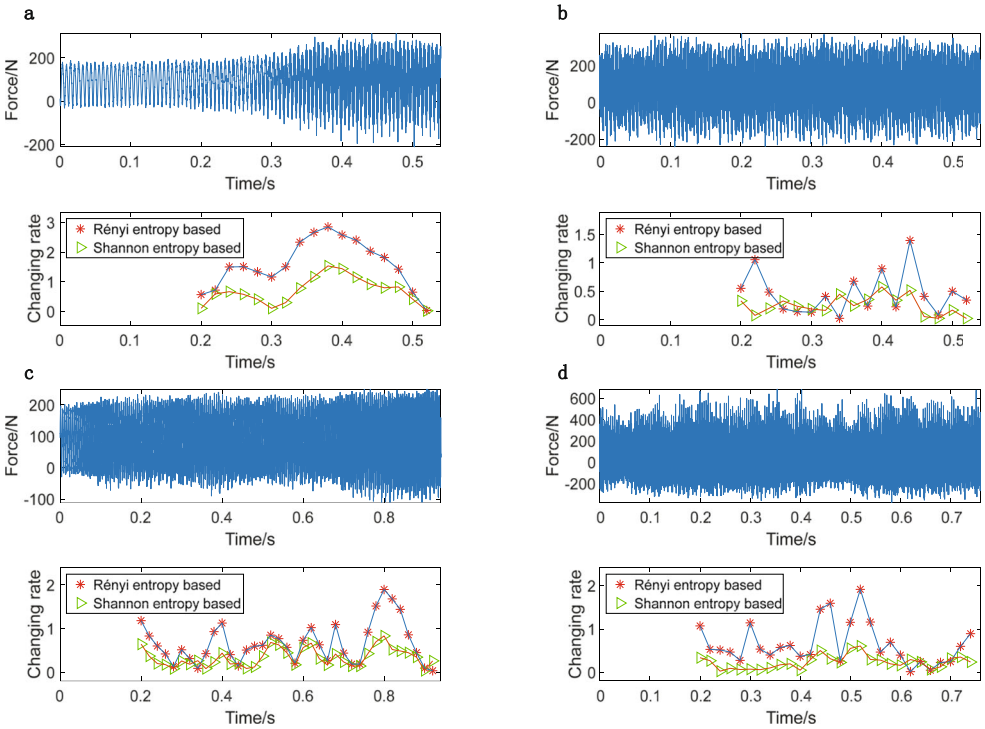

Fig. 12 The absolute changing rates of the Rényi entropy and Shannon entropy indicators values in the transition period of different cases. **a** Case 1. **b** Case 2. **c** Case 3. **d** Case 4

To make the threshold lie in the range [0,1] and independent of the cutting condition, the alarm value is normalized as follows:

$$Threshold = \frac{Initial\_value - Alarm\_value}{Initial\_value - Final\_value} \quad (15)$$

As displayed in Fig. 14, the Rényi entropy-based indicator can always detect the chatter earlier in the transition period with the same threshold, which indicates its better agility in identifying the chatter at an early stage.

4.6 Comparison with a time-frequency domain method

In this subsection, another commonly used method based on the time-frequency domain analysis [16] is

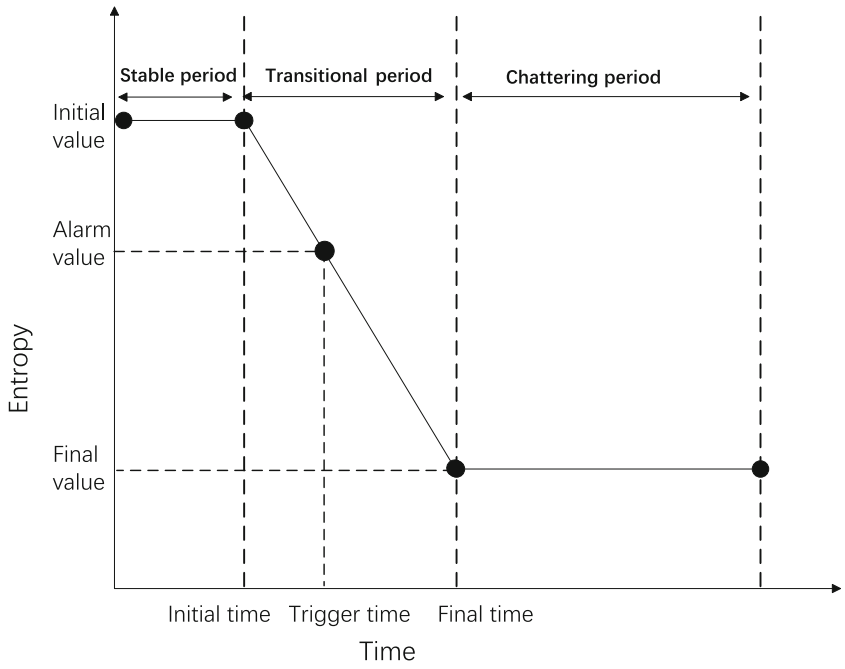

Fig. 13 The schematic diagram of the entropy based indicator in milling processes

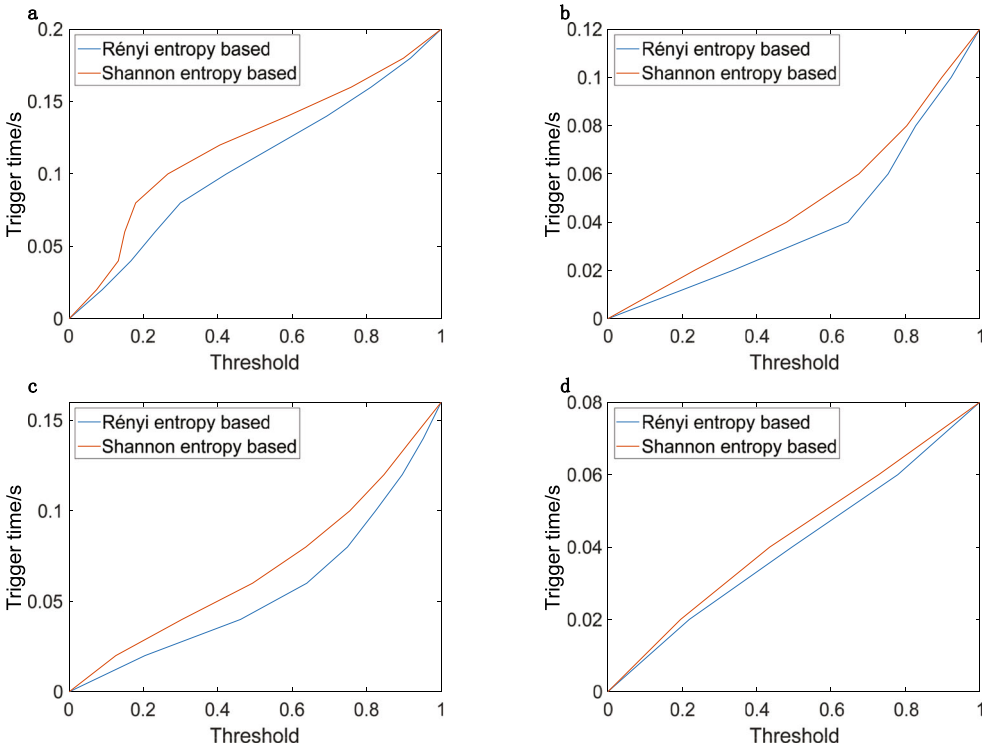

Fig. 14 The chatter trigger time of different preseted thresholds in tests **a** Case 1. **b** Case 2. **c** Case 3. **d** Case 4

compared with the proposed method. In that method, the signals are preprocessed with the WPT and HHT first. Then, the mean value (MV) and standard deviation (SD) of the Hilbert–Huang spectrum are defined as the indicators. The three indicators, namely the Rényi entropy, MV and SD, are calculated with the data collected in Case 1 and illustrated in Fig. 15. It can be seen that all of these indicators show that significant changes at the onset of the chatter and the changing moments, which can be considered as the time when the chatter is identified, are almost the same. In order to evaluate the changing moment quantitatively, the 3σ rule is

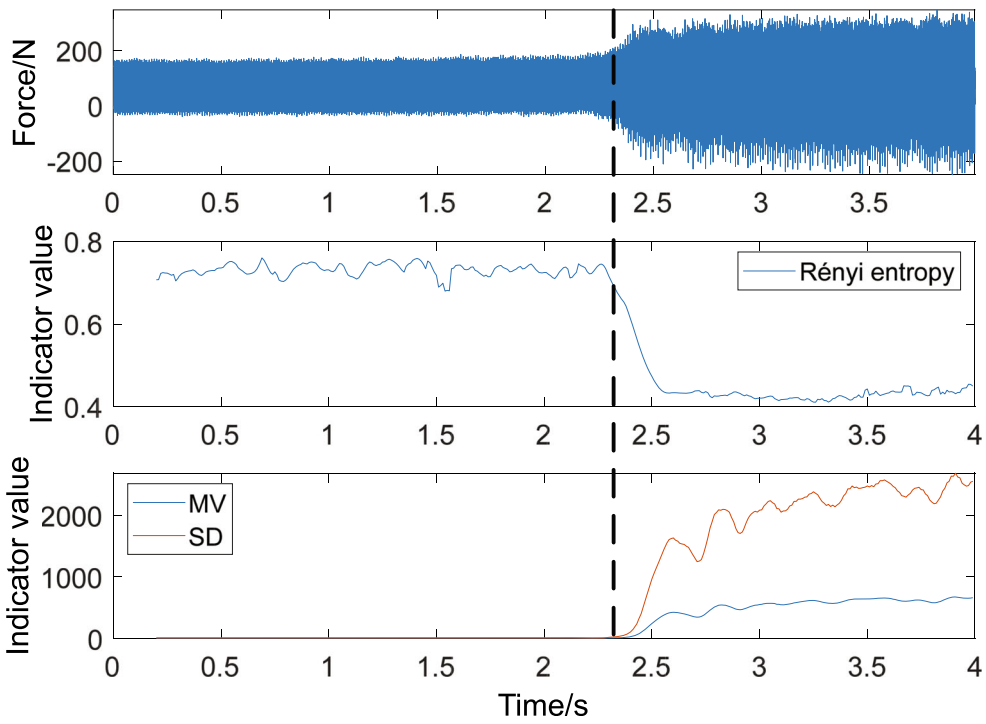

Fig. 15 **a** The force signal of Case 1 in the time domain. **b** The Rényi entropy indicator value of the force signal. **c** The MV and SD values of the force signal.

applied, which is commonly used in the machinery health prognostics [33]. The indicator values between 0 s and 1.5 s, corresponding to the stable status, are selected to calculate the mean and standard deviation first. Then, the changing moment can be determined as the time that the indicator value deviates from the mean value more than 3σ. The calculation results of these three indicators are 2.34 s, 2.30 s, and 2.29 s, respectively. It can be seen that the difference among the results is tiny, just 50 ms, which indicates the comparable capability of the proposed method in chatter identification. The proposed method shows advantages in other aspects. First, as pointed out by Cao et al. [16], the wavelet packet used in the time-frequency analysis is selected based on the experience. However, the distribution of the chatter frequencies is very complicated in practice and could not be determined in advance. With the proposed Rényi entropy indicator, there is no requirement of the chatter frequencies. Second, the proposed MV indicator is affected by the cutting parameters; thus, the threshold for detecting the chatter needs to be adjusted once the cutting conditions are changed. However, the Rényi entropy is a dimensionless indicator and only depends on the severity of the chatter.

5 Conclusion

This paper proposes a practical method to identify the chatter in milling processes. Since the energy of the chatter signal gradually gather at the chatter frequencies when the chatter severity level grows, the frequency-domain Rényi entropy is proposed as a chatter indicator. The method is validated with milling experiments. The results show that the Rényi entropy-based indicator identifies different milling states successfully and detects the chatter at quite an early stage under various milling conditions. The indicator is also compared with the commonly used Shannon entropy based one and verified to possess a larger variation range, higher sensitivity to the chatter onset and better agility to detect chatter at the early stage. The comparison with a time-frequency domain method also shows its comparable capability in chatter monitoring. Meanwhile, it is worth mentioning that since only the FFT is applied in signal preprocessing, the indicator needs not to specify any additional parameters and is computationally efficient. However, it is also noticed that the method to obtain the accurate indicator thresholds for chatter identification which satisfy various requirements in industry still needs to be explored.

Funding information This work is supported by the National Natural Science Foundation of China (Grant No. 91648202 and No.51905345).

References

1. Budak E, Altintaş Y (1998) Analytical Prediction of Chatter Stability in Milling—Part II: Application of the General Formulation to Common Milling Systems. J Dyn Syst Meas Control 120:31–36. https://doi.org/10.1115/1.2801318
2. Quintana G, Ciurana J (2011) Chatter in machining processes : A review. Int J Mach Tools Manuf 51:363–376. https://doi.org/10.1016/j.ijmachtools.2011.01.001
3. Yang K, Wang G, Dong Y et al (2019) Early chatter identification based on an optimized variational mode decomposition. Mech Syst Signal Process 115:238–254. https://doi.org/10.1016/j.ymssp.2018.05.052
4. Ji Y, Wang X, Liu Z et al (2018) Early milling chatter identification by improved empirical mode decomposition and multi-indicator synthetic evaluation. J Sound Vib 433:138–159. https://doi.org/10.1016/j.jsv.2018.07.019
5. Ding L, Sun Y, Xiong Z (2017) Early chatter detection based on logistic regression with time and frequency domain features. IEEE/ASME International Conference on Advanced Intelligent Mechatronics, AIM 1052–1057. https://doi.org/10.1109/AIM.2017.8014158
6. Wang Y, Bo Q, Liu H, Hu L, Zhang H (2018) Mirror milling chatter identification using Q-factor and SVM. Int J Adv Manuf Technol 98:1163–1177. https://doi.org/10.1007/s00170-018-2318-x
7. Liu H, Chen Q, Li B et al (2011) On-line chatter detection using servo motor current signal in turning. Sci China Technol Sci 54:3119–3129. https://doi.org/10.1007/s11431-011-4595-6
8. Hynynen KM, Ratava J, Lindh T et al (2014) Chatter Detection in Turning Processes Using Coherence of Acceleration and Audio Signals. J Manuf Sci Eng 136:044503. https://doi.org/10.1115/1.4026948
9. Caliskan H, Kilic ZM, Altintas Y (2018) On-Line Energy-Based Milling Chatter Detection. J Manuf Sci Eng 140:111012. https://doi.org/10.1115/1.4037849
10. Ye J, Feng P, Xu C, Ma Y, Huang S (2018) A novel approach for chatter online monitoring using coefficient of variation in machining process. Int J Adv Manuf Technol 96:287–297. https://doi.org/10.1007/s00170-017-1544-y
11. Lajmert P, Rusinek R, Kruszyński B (2018) Chatter identification in milling of Inconel 625 based on recurrence plot technique and Hilbert vibration decomposition. MATEC Web of Conferences 148:09003. https://doi.org/10.1051/matecconf/201814809003
12. Jia G, Wu B, Hu Y, Xie FY, Liu A (2013) A synthetic criterion for early recognition of cutting chatter. Sci China Technol Sci 56:2870–2876. https://doi.org/10.1007/s11431-013-5360-9
13. Zhang Z, Li H, Meng G et al (2016) Chatter detection in milling process based on the energy entropy of VMD and WPD. Int J Mach Tools Manuf 108:106–112. https://doi.org/10.1016/j.ijmachtools.2016.06.002
14. Zhang C (2009) Cutting Chatter Monitoring Using Hidden Markov Models. Control, Automation and Systems Engineering, 2009 CASE 2009 IITA International Conference on IEEE 504–507. https://doi.org/10.1109/CASE.2009.63
15. Shao Q, Feng CJ, Li W (2011) Hybrid PCA-SVM method for pattern recognition of chatter gestation. Proceedings of the 2011 2nd International Conference on Digital Manufacturing and Automation, ICDMA 2011 598–601. https://doi.org/10.1109/ICDMA.2011.149
16. Cao H, Lei Y, He Z (2013) Chatter identification in end milling process using wavelet packets and Hilbert-Huang transform. Int J Mach Tools Manuf 69:11–19. https://doi.org/10.1016/j.ijmachtools.2013.02.007

17. Cabrera CG, Araujo AC, Castello DA (2017) On the wavelet analysis of cutting forces for chatter identification in milling. Adv Manuf 5:130–142. https://doi.org/10.1007/s40436-017-0179-4
18. Huang NE, Shen Z, Long SR et al (1998) The empirical mode decomposition and the Hilbert spectrum for nonlinear and non-stationary time series analysis. Proceedings of the Royal Society of London Series A: mathematical, physical and engineering sciences 454:903–995. https://doi.org/10.1098/rspa.1998.0193
19. Fu Y, Zhang Y, Zhou H et al (2016) Timely online chatter detection in end milling process. Mech Syst Signal Process 75:668–688. https://doi.org/10.1016/j.ymssp.2016.01.003
20. Wan S, Li X, Chen W, Hong J (2018) Investigation on milling chatter identification at early stage with variance ratio and Hilbert–Huang transform. Int J Adv Manuf Technol 95:3563–3573. https://doi.org/10.1007/s00170-017-1410-y
21. Liu C, Zhu L, Ni C (2017) The chatter identification in end milling based on combining EMD and WPD. Int J Adv Manuf Technol 91:3339–3348. https://doi.org/10.1007/s00170-017-0024-8
22. Wei C, Liu M, Huang G (2016) Chatter Identification of Face Milling Operation via Time-Frequency and Fourier Analysis. International Journal of Automation and Smart Technology 6:25–36. https://doi.org/10.5875/ausmt.v6i1.1018
23. Cao H, Zhou K, Chen X (2015) Chatter identification in end milling process based on EEMD and nonlinear dimensionless indicators. Int J Mach Tools Manuf 92:52–59. https://doi.org/10.1016/j.ijmachtools.2015.03.002
24. Chen GS, Zheng QZ (2018) Online chatter detection of the end milling based on wavelet packet transform and support vector machine recursive feature elimination. Int J Adv Manuf Technol 95:775–784. https://doi.org/10.1007/s00170-017-1242-9
25. Yao Z, Mei D, Chen Z (2010) On-line chatter detection and identification based on wavelet and support vector machine. J Mater Process Technol 210:713–719. https://doi.org/10.1016/j.jmatprotec.2009.11.007
26. Han Z, Jin H, Han D, Fu H (2017) ESPRIT- and HMM-based real-time monitoring and suppression of machining chatter in smart CNC milling system. Int J Adv Manuf Technol 89:2731–2746. https://doi.org/10.1007/s00170-016-9863-y
27. Lamraoui M, Barakat M, Thomas M, El Badaoui M (2015) Chatter detection in milling machines by neural network classification and feature selection. J Vib Control 21:1251–1266. https://doi.org/10.1177/1077546313493919
28. Altintas Y, Stepan G, Merdol D, Dombovari Z (2008) Chatter stability of milling in frequency and discrete time domain. CIRP J Manuf Sci Technol 1:35–44. https://doi.org/10.1016/j.cirpj.2008.06.003
29. Ma L, Melkote SN, Castle JB (2013) A Model-Based Computationally Efficient Method for On-Line Detection of Chatter in Milling. J Manuf Sci Eng 135:031007–031007-11. https://doi.org/10.1115/1.4023716
30. Tao B, Zhu L, Ding H, Xiong Y (2007) An alternative time-domain index for condition monitoring of rolling element bearings-A comparison study. Reliab Eng Syst Saf 92:660–670. https://doi.org/10.1016/j.ress.2006.03.005
31. Liu C, Zhu L, Ni C (2018) Chatter detection in milling process based on VMD and energy entropy. Mech Syst Signal Process 105:169–182. https://doi.org/10.1016/j.ymssp.2017.11.046
32. Ji Y, Wang X, Liu Z, Yan Z, Jiao L, Wang D, Wang J (2017) EEMD-based online milling chatter detection by fractal dimension and power spectral entropy. Int J Adv Manuf Technol 92:1185–1200. https://doi.org/10.1007/s00170-017-0183-7
33. Lei Y, Li N, Guo L et al (2018) Machinery health prognostics : A systematic review from data acquisition to RUL prediction Machinery health prognostics : A systematic review from data acquisition to RUL prediction. Mech Syst Signal Process 104:799–834. https://doi.org/10.1016/j.ymssp.2017.11.016